# Radiation From an Aperture in a Coated Plane[1]

## Charles M. Knop [2] and George I. Cohn [3]

In this paper the method developed by J. R. Wait to determine the fields produced by an aperture in an infinite coated-metal cylinder is extended to obtain the solution for the fields produced by an aperture in an infinite coated-metal plane. Although the fields at any point can be found by this method, this paper treats only the radiation fields (a future paper is planned which will treat the near fields and input admittance of the aperture). It is shown that the radiation fields produced by a given aperture for the coated case are related to those of the uncoated case, for the same aperture excitation, by simple multiplicative functions which depend only on the parameters of the coating and the off-axis angle. These findings, combined with experimental results for finite size uncoated and coated plates in conjunction with semi-empirical and empirical theories, respectively, are then generalized to obtain the radiation fields produced by a slot in a coated finite metal plate. The sharpening and broadening effects on the radiation patterns due to a lossless plasma coating are also obtained from the general solution.

## List of Symbols

$\mathbf{E}$=vector electric field intensity, volts/meter

$\mathbf{H}$=vector magnetic field intensity, amperes/meter

$\mathrm{E_x}$=$x$ component of $\mathbf{E}$, etc.

$\bar{f}$=double Fourier transform of the function $f(x, y)$

$\bar{F}^{-1}$=double inverse Fourier transform operator

$\overline{E_1^+}$=double Fourier transform of forward going axial electric field in region 1, etc.

$\overline{E_1^-}$=double Fourier transform of backward going axial electric field in region 1, etc.

$c$=cosine

$s$=sine

$\beta_v=\omega\sqrt{\mu_v\epsilon_v}=2\pi/\lambda_v$=phase factor in vacuum

$\mu_v$=permeability of vacuum=$4\pi\cdot10^{-7}$ henries/meter

$\epsilon_v$=permittivity of vacuum=$1/36\pi\cdot10^9$ farads/meter

$\lambda_v$=wavelength of source in vacuum

$\gamma_1$=propagation factor in coating

$\beta_2$=phase factor in region external to coating

$\beta_c^2=\xi^2+\eta^2$=square of cutoff phase factor=$\begin{cases} \beta_v^2 \overset{v}{\mu_r}\overset{v}{\epsilon_r}+\gamma_1^2 \text{ in coating} \\ \beta_v^2-\beta_2^2 \text{ in region external to coating} \end{cases}$

$\xi$=wave number in $x$ direction

$\eta$=wave number in $y$ direction

$\overset{v}{\mu_r}$=complex relative permeability of coating

$\overset{v}{\epsilon_r}$=complex relative dielectric constant of coating

$d$=thickness of coating

$f_p=\omega_p/2\pi$=plasma frequency $\approx 9\sqrt{n}$ cycles/second

$n$=electron density, electron/meter$^3$

(All other symbols are defined as they are introduced.)

---

[2] NESCO, Pasadena, Calif.; formerly with The Hallicrafters Company, Chicago, Ill.
[3] Consultant; formerly Professor of Electrical Engineering, Illinois Institute of Technology, Chicago, Ill.

# 1. Introduction

In this paper the method previously developed to determine the radiation fields from an aperture in a coated cylinder [Wait and Mientka, 1957; Wait and Conda, 1957b; Wait, 1959] is extended to obtain the solution for the radiation fields produced by an aperture in a coated plane. In particular, the radiation structure considered is an infinite perfectly conducting plane with an arbitrarily shaped aperture excited by a specified tangential, electric field distribution. The entire plane is covered by a material coating of complex dielectric constant $\overset{v}{\epsilon_1}=\overset{v}{\epsilon_v}\epsilon_{r'}$ complex permeability $\overset{v}{\mu_1}=\mu_v\overset{v}{\mu_{r'}}$ and thickness $d$. The structure is depicted in figure 1a.
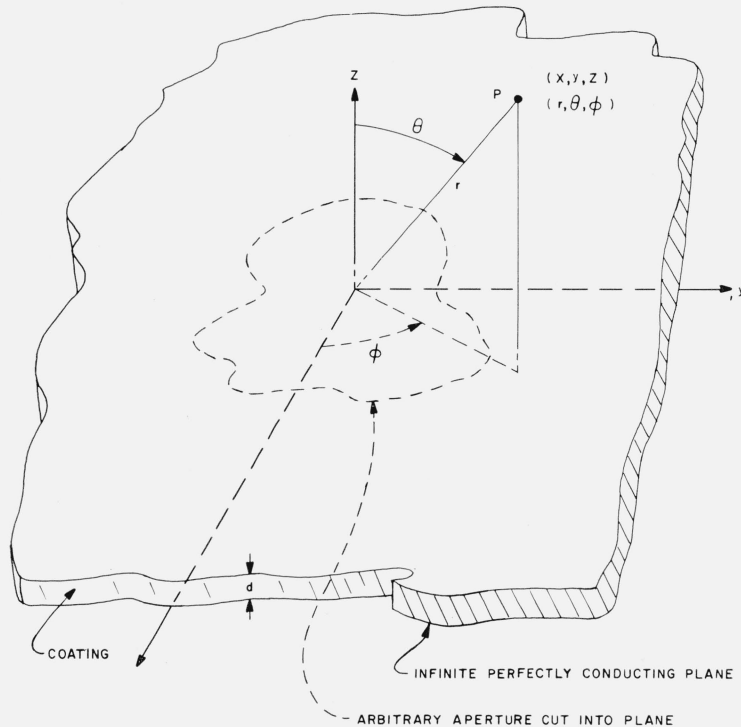


FIGURE 1a. *Arbitrary aperture cut in a coated perfectly conducting plane.*

# 2. Formal Solution

The fields produced by the specified tangential, electric field distribution are found by solving a two-region boundary value problem. These regions are region $1: 0 \leq z \leq d$ and region $2: d \leq z \leq \infty$. To solve for the fields the method of Wait is used. First, from Maxwell's equations it can be shown that the axial $(z)$ components of both the $\mathbf{E}$ and $\mathbf{H}$ fields in each region obey the scalar wave equation for that region, namely $\nabla^2\psi + \beta_c^2\psi = 0$ where $\psi$ can represent any of the axial components of either the electric or magnetic fields in either region. The propagation in region 1 is taken as $e^{\pm\gamma_1 z}$ and in region 2 as $e^{-j\beta_2 z}$. The solution for $\psi$ is expressed as a double Fourier integral over mode space, i.e., the axial fields are expressed as inverse Fourier transforms. The transverse fields are then found from Maxwell's equations and the assumed propagation. This process gives for the fields in region 1

$$E_z = \overline{F}^{-1}[\overline{E}_1^+ e^{-\gamma_1 z} + \overline{E}_1^- e^{\gamma_1 z}]$$

$$H_z = \overline{F}^{-1}[\overline{H}_1^+ e^{-\gamma_1 z} + \overline{H}_1^- e^{\gamma_1 z}]$$

$$E_x = \overline{F}^{-1}\left\{ \frac{e^{-\gamma_1 z}}{(\xi^2+\eta^2)}\left[-j\gamma_1\xi\overline{E}_1^+ + \omega\overset{v}{\mu}_1\eta\overline{H}_1^+\right] + \frac{e^{\gamma_1 z}}{(\xi^2+\eta^2)}\left[j\gamma_1\xi\overline{E}_1^- + \omega\overset{v}{\mu}_1\eta\overline{H}_1^-\right]\right\}$$

$$E_y = \overline{F}^{-1}\left\{ \frac{e^{-\gamma_1 z}}{(\xi^2+\eta^2)}\left[-j\gamma_1\eta\overline{E}_1^+ - \omega\overset{v}{\mu}_1\xi\overline{H}_1^+\right] + \frac{e^{\gamma_1 z}}{(\xi^2+\eta^2)}\left[+j\gamma_1\eta\overline{E}_1^- - \omega\overset{v}{\mu}_1\xi\overline{H}_1^-\right]\right\}$$ (1)

$$H_x = \overline{F}^{-1}\left\{ \frac{e^{-\gamma_1 z}}{(\xi^2+\eta^2)}\left[-\omega\overset{v}{\epsilon}_1\eta\overline{E}_1^+ - j\gamma_1\xi\overline{H}_1^+\right] + \frac{e^{\gamma_1 z}}{(\xi^2+\eta^2)}\left[-\omega\overset{v}{\epsilon}_1\eta\overline{E}_1^- + j\gamma_1\xi\overline{H}_1^-\right]\right\}$$

$$H_y = \overline{F}^{-1}\left\{ \frac{e^{-\gamma_1 z}}{(\xi^2+\eta^2)}\left[\omega\overset{v}{\epsilon}_1\xi\overline{E}_1^+ - j\gamma_1\eta\overline{H}_1^+\right] + \frac{e^{\gamma_1 z}}{(\xi^2+\eta^2)}\left[\omega\overset{v}{\epsilon}_1\xi\overline{E}_1^- + j\gamma_1\eta\overline{H}_1^-\right]\right\}$$

and for those in region 2,

$$E_z = \overline{F}^{-1}[\overline{E}_2 e^{-i\beta_2 z}]$$

$$H_z = \overline{F}^{-1}[\overline{H}_2 e^{-i\beta_2 z}]$$

$$E_x = \overline{F}^{-1}\left\{ \frac{e^{-i\beta_2 z}}{(\xi^2+\eta^2)}\left[\beta_2\xi\overline{E}_z + \omega\mu_v\eta\overline{H}_2\right]\right\}$$

$$E_y = \overline{F}^{-1}\left\{ \frac{e^{-i\beta_2 z}}{(\xi^2+\eta^2)}\left[\beta_2\eta\overline{E}_2 - \omega\mu_v\xi\overline{H}_2\right]\right\}$$ (2)

$$H_x = \overline{F}^{-1}\left\{ \frac{e^{-i\beta_2 z}}{(\xi^2+\eta^2)}\left[-\omega\epsilon_v\eta\overline{E}_2 + \beta_2\xi\overline{H}_2\right]\right\}$$

$$H_y = \overline{F}^{-1}\left\{ \frac{e^{-i\beta_2 z}}{(\xi^2+\eta^2)}\left[\omega\epsilon_v\xi\overline{E}_2 + \beta_2\eta\overline{H}_2\right]\right\}$$

where the argument $(x, y, z)$ of the fields is understood. In the above the Fourier transform symbols

$$\overline{F}^{-1}[\overline{f}(\xi,\eta)] = \int_{-\infty}^{\infty}\int_{-\infty}^{\infty}\overline{f}(\xi,\eta)e^{j(\xi x+\eta y)}dxdy = f(x,y)$$ (3)

$$\overline{f}(\xi,\eta) = \frac{1}{(2\pi)^2}\int_{-\infty}^{\infty}\int_{-\infty}^{\infty}f(x,y)e^{-j(\xi x+\eta y)}dxdy$$ (4)

are used. It should be noted here that the above formal representation of the fields as inverse Fourier transforms can be established on a rigorous physical basis by initially considering the given coated aperture exciting a hypothetical square metal waveguide of wall spacing $L$ and of infinite length. The axial and transverse fields for a finite $L$ are expressed in a double Fourier series as for an ordinary waveguide. The walls are then displaced to infinity and the Fourier series expressions for the fields become Fourier integrals. This procedure converts the discrete mode spectrum into one which is continuous [Cohn and Flesher, 1958] and has been previously applied to the coated cylinder [Knop, 1961]. Equations (1) and (2) contain the six unknown Fourier mode spectrum coefficients $\overline{E}_1^+$, $\overline{E}_1^-$, $\overline{H}_1^+$, $\overline{H}_1^-$, $\overline{E}_2$, and $\overline{H}_2$. These are found by applying the tangential boundary conditions at the surfaces $z=d$ and $z=0$. These are the equality of the corresponding $E_x$, $H_x$, $E_y$, and $H_y$ fields in each region to each other at $z=d$; and the specified fields at $z=0$, namely

$$E_{x1}(x,\,y,\,0)=\begin{cases} E_x^A(x,y) & \text{on aperture} \\ 0 & \text{off aperture} \end{cases} \tag{5}$$

$$E_{y1}(x,\,y,\,0)=\begin{cases} E_y^A(x,y) & \text{on aperture} \\ 0 & \text{off aperture} \end{cases} \tag{6}$$

where $E_x^A(x,\,y)$ and $E_y^A(x,\,y)$ are the specified aperture $x$ and $y$ components of electric fields. Using (1) with (5) and (6) gives

$$\overline{E}_x^A(\xi,\,\eta)\equiv\frac{1}{4\pi^2}\iint\limits_{A_p} e^{-j(\xi x+\eta y)}E_x^A(x,y)dxdy=\frac{1}{(\xi^2+\eta^2)}\left[-j\gamma_1\xi(\overline{E}_1^+-E_1^-)+\omega\overset{v}{\mu}_1(\overline{H}_1^++\overline{H}_1^-)\right] \tag{7}$$

$$\overline{E}_y^A(\xi,\,\eta)\equiv\frac{1}{4\pi^2}\iint\limits_{A_p} e^{-j(\xi x+\eta y)}E_y^A(x,y)dxdy=\frac{1}{(\xi^2+\eta^2)}\left[-\omega\overset{v}{\mu}_1\xi(\overline{H}_1^++\overline{H}_1^-)-j\gamma_1\eta(\overline{E}_1^+-\overline{E}_1^-)\right] \tag{8}$$

where $A_p$ means integration over the aperture. Use of the four boundary conditions at $z=d$ with (1) and (2) then gives with (7) and (8) a set of six equations in the six unknowns $\overline{E}_1^+$, etc., in terms of the excitation factors $\overline{E}_x^A(\xi,\,\eta)$ and $\overline{E}_y^A(\xi,\eta)$. To find the radiation fields it suffices to find $\overline{E}_2$ and $\overline{H}_2$. However, before solving for these coefficients, it is noted that all the field components in region 2 can be written in the form

$$g(x,\,y,\,z)=\overline{F}^{-1}[\overline{g}(\xi,\eta)e^{-j\beta_2 z}] \tag{9}$$

where $g(x,\,y,\,z)=E_{x2},\,E_{y2}$, etc., and $\overline{g}(\xi,\,\eta)$ is the corresponding factor appearing in the inverse Fourier transform of (2). This inverse Fourier transform operation is greatly facilitated in the radiation zone (i.e., for large $r$) by successive application of the method of stationary phase [Di Francia, 1955] and gives

$$g(x,\,y,\,z)=A\overline{g}(\xi_0,\,\eta_0)c\theta+0(r^{-n}),\qquad n>1 \tag{10}$$

where $A=j2\pi\beta_v e^{-j\beta_v r}/r$, $\xi_0=-\beta_v s\theta c\phi$, and $\eta_0=-\beta_v s\theta s\phi$. Thus, to determine the radiation fields (the fields of order $1/r$) it is only necessary to determine $\overline{g}(\xi,\,\eta)$ at the modal point $(\xi_0,\,\eta_0)$.

At this point $\gamma_1=\alpha_1+j\beta_1=\pm j\beta_v\sqrt{\overset{v}{\mu}_r\overset{v}{\epsilon}_r-s^2\theta}$, where the sign on the radical is chosen so as to make $\alpha_1\geq 0$ and $\beta_1\geq 0$ so as to have physically realizable waves in the passive media. The radiation fields then become, using (10) in (2) and changing to spherical coordinates (dropping the subscript 2 and understanding radiation fields only)

$$E_r=H_r=0 \tag{11}$$

$$E_\theta=\sqrt{\frac{\mu_v}{\epsilon_v}}\,H_\phi=-A\cot\theta\overline{E}_2(\xi_0,\,\eta_0) \tag{12}$$

$$E_\phi=-\sqrt{\frac{\mu_v}{\epsilon_v}}\,H_\theta=A\cot\theta\sqrt{\frac{\mu_v}{\epsilon_v}}\,\overline{H}_2(\xi_0,\,\eta_0). \tag{13}$$

Evaluating $\overline{E}_2(\xi_0,\,\eta_0)$ and $\overline{H}_2(\xi_0,\,\eta_0)$ from the previously mentioned six equations in six unknowns using determinants, and substituting in (12) and (13) gives (after some algebra)

$$E_\theta=Af(\theta)[\overline{E}_x^0 c\phi+\overline{E}_y^0 s\phi] \tag{14}$$

$$E_\phi=Ag(\theta)[-\overline{E}_x^0 s\phi+\overline{E}_y^0 c\phi]c\theta \tag{15}$$

where $\bar{E}_x^0$ and $\bar{E}_y^0$ are $\bar{E}_x^A$ and $\bar{E}_y^A$, respectively, evaluated at $(\xi_0, \eta_0)$, and where

$$g(\theta) = e^{j\beta_v dc\theta}/[c\dot{\psi} + jz_E s\psi] \tag{16}$$

$$f(\theta) = e^{j\beta_v dc\theta}/[c\psi + jz_H s\psi] \tag{17}$$

with $\psi$=electrical length of coating material$= -j\gamma_1 d = \beta_v d\sqrt{\overset{v}{\mu_r}\overset{v}{\epsilon_r} - s^2\theta}$, $z_H = \sqrt{\overset{v}{\mu_r}\overset{v}{\epsilon_r} - s^2\theta}/\overset{v}{\epsilon_r}c\theta$, and $z_E = \overset{v}{\mu_r}c\theta/\sqrt{\overset{v}{\mu_r}\overset{v}{\epsilon_r} - s^2\theta}$. Equations (14) and (15) constitute the exact solution for the radiation fields produced by a specified tangential, electric field distribution in an arbitrarily shaped aperture cut in a perfectly conducting plane coated with a dielectric-permeable slab having a complex relative dielectric constant, $\overset{v}{\epsilon_r}$, a complex relative permeability $\overset{v}{\mu_r}$, and of thickness $d$.

### 2.1. Special Case of Uncoated Plane

As a partial check on the above solution, consider the case of an uncoated plane, i.e., either a vanishing coating thickness, $d=0$, or a slab of free space $\overset{v}{\mu_r} = \overset{v}{\epsilon_r} = 1$. In either case $g(\theta)$ and $f(\theta)$ become unity.

$$g(\theta) = f(\theta) = 1 \text{ for } d=0 \text{ and/or } \overset{v}{\mu_r} = \overset{v}{\epsilon_r} = 1. \tag{18}$$

The radiation fields for the uncoated case are then given by (14) and (15) with (18). The use of these equations for the radiation fields gives results which are identical to those obtained by solving the given problem by other methods.

### 2.2. Relation Between Radiation Fields From Uncoated and Coated Apertures

From (18), (14), and (15) the radiation fields from an aperture with a coating can be expressed in terms of those without the coating, for the same aperture excitation, by the multiplicative factors $g(\theta)$ and $f(\theta)$, which for a given frequency, only depend on the off axis angle, $\theta$, and the parameters of the coating. Thus,

$$E_\theta\big|_{\text{with coating}} = f(\theta)E_\theta\big|_{\text{no coating}}, \quad E_\phi\big|_{\text{with coating}} = g(\theta)E_\phi\big|_{\text{no coating}} \tag{19}$$

It is to be stressed that (19) holds only if the tangential electric field distribution over the aperture is the same with and without the coating. If this is not true, then (14) and (15) must be used individually for each case.

### 2.3. The Radiation Fields From a Rectangular Slot

Consider the rectangular slot depicted in figure 1b and excited as follows:

$$\bar{E}_x^A(x,y) = 0, \quad \bar{E}_y^A(x,y) = E_0 s[\beta_v(x_0/2 - |x|)] \tag{20}$$

which give $\bar{E}_x^0 = 0$, $\bar{E}_y^0 = V_0 P(\theta,\phi)/2\pi^2\beta_v$, where $V_0 = E_0 y_0$, and $P(\theta,\phi) = \{c[(\beta_v x_0/2)s\theta c\phi] - c(\beta_v x_0/2)\}/\{1 - s^2\theta c^2\phi\}$, and where the restriction that a thin slot (i.e., $s[(\beta_v y_0/2)s\theta s\phi]/(\beta_v y_0/2)s\theta s\phi \approx 1$) has been made. From (14), (15), and (18), the radiation fields from this slot for the no coating case are

$$E_\theta = AV_0 P(\theta,\phi)s\phi/2\pi^2\beta_v, \quad E_\phi = AV_0 P(\theta,\phi)c\theta c\phi/2\pi^2\beta_v. \tag{21}$$

For the coating case and the same excitation the radiation fields are given by (19) and (21) with (16) and (17).

## 3. Numerical Computations—Teflon Coated Slot

Calculations of the radiation patterns for the case of a thin rectangular half wavelength slot $\left(\beta_v\dfrac{x_0}{2} = \dfrac{\pi}{2}\right)$ coated with a material having a practically lossless dielectric constant,
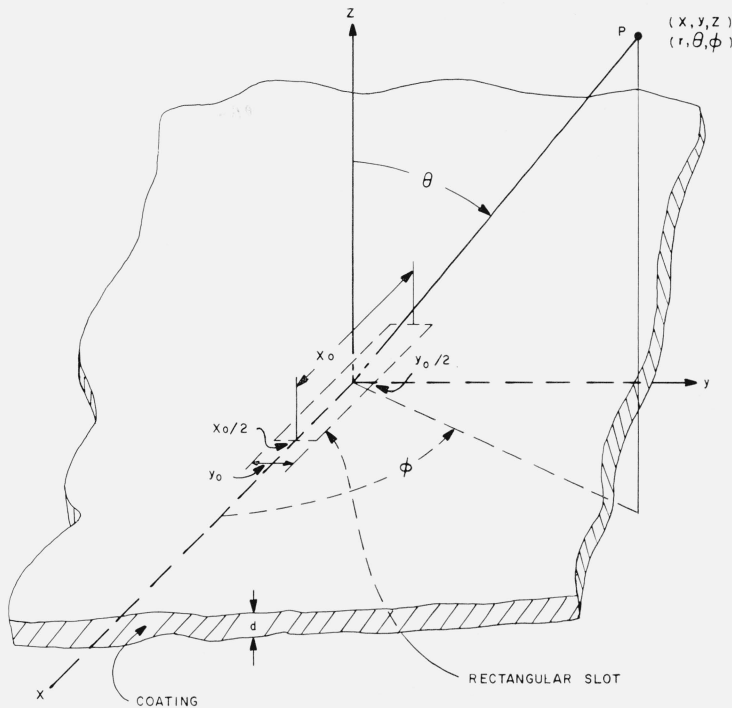
FIGURE 1b. *Rectangular slot cut in a coated perfectly conducting plane.*

$\overset{v}{\epsilon}_r = \epsilon'_r = 2.10$ (Teflon) for the cases of a thin $\left(\dfrac{d}{\lambda_v} = 0.10\right)$, a medium $\left(\dfrac{d}{\lambda_v} = 0.40\right)$, and a thick $\left(\dfrac{d}{\lambda_v} = 2.39\right)$, coating were made. The patterns were calculated for the principal planes only, i.e., the horizontal $xz$=plane ($\phi=0$, $\theta$ variable) and the vertical, i.e., $yz$ plane ($\phi=\pi/2$, $\theta$ variable). These patterns are obtained from (21) with $P(\theta,0)=c[(\pi/2)s\theta]/c^2\theta$, and $P(\theta,\pi/2)=1$, and are $E_\phi(r,\theta,0)=jV_0c[(\pi/2)s\theta]e^{-j\beta_v r}g(\theta)/r\pi c\theta$, $E_\theta(r,\theta,0)=0$, and $E_\theta(r,\theta,\pi/2)=jV_0e^{-j\beta_v r}f(\theta)/r\pi$, $E_\phi(r,\theta,\pi/2)=0$, with $f(\theta)$ and $g(\theta)$ given by (16) and (17). All patterns are symmetrical $WRT$ $\theta$. The radiation power patterns in decibels in these planes $\left(\text{plots of } 20\log_{10}\left|\dfrac{E_\theta(0,\pi/2)}{E_\theta(\theta,\pi/2)}\right|\right.$ and $20\log_{10}\left|\dfrac{E_\phi(0,0)}{E_\phi(\theta,0)}\right|\left.\right)$ in decibels are shown in figure 2. The patterns for the noncoated slot are also shown. These patterns show that the thin and medium thickness coatings have a very slight effect on the horizontal plane patterns. However, the thick coating broadens the pattern and introduces a lobe, less than a db down, at approximately 61° off the axis. It is also noted that for all the coatings the field in the horizontal plane near the dielectric coated ground plane ($\theta \approx 90°$) approaches zero, as is the case for no coating present.

For the vertical plane radiation pattern, figure 2b reveals that near the axis ($\theta=0°$) the thin and medium coatings produce a slight effect, but as $\theta$ approaches $\pm 90°$ the electric field approaches zero, indicating that with even the thin coating the radiation can be significantly reduced in this plane for angles near the ground plane. The thick coating again has the effect of broadening the radiation near the axis, but also causes it to approach zero (although not as soon as the thin and medium coatings) at angles near the ground plane. This is to be compared with the noncoated case where the electric field in the vertical plane is constant. It is to be stressed that these patterns are for an infinite ground plane. Their adequacy to describe the radiation from a finite ground plane will be discussed shortly.

368

FIGURE 2a.  *Calculated power radiation patterns in horizontal (xz) plane of a dielectric coated slot antenna.*
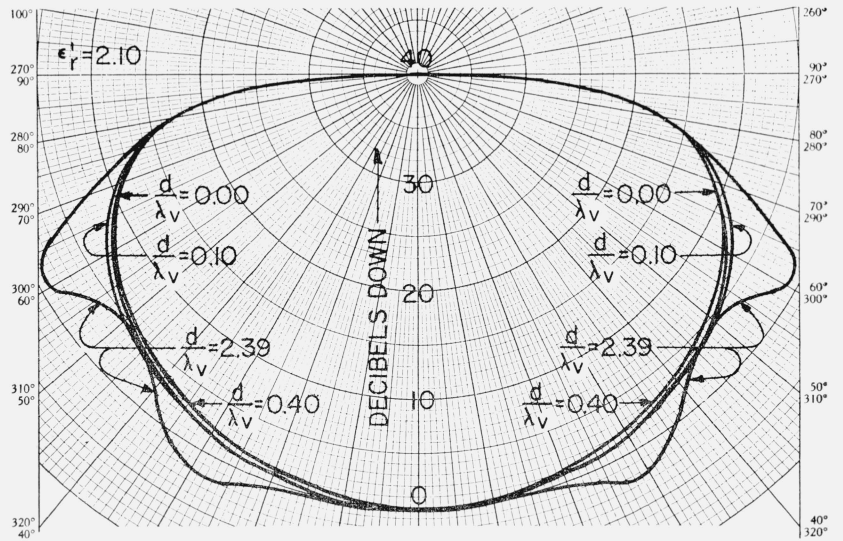


FIGURE 2b.  *Calculated power radiation patterns in vertical (yz) plane of a dielectric coated slot antenna.*
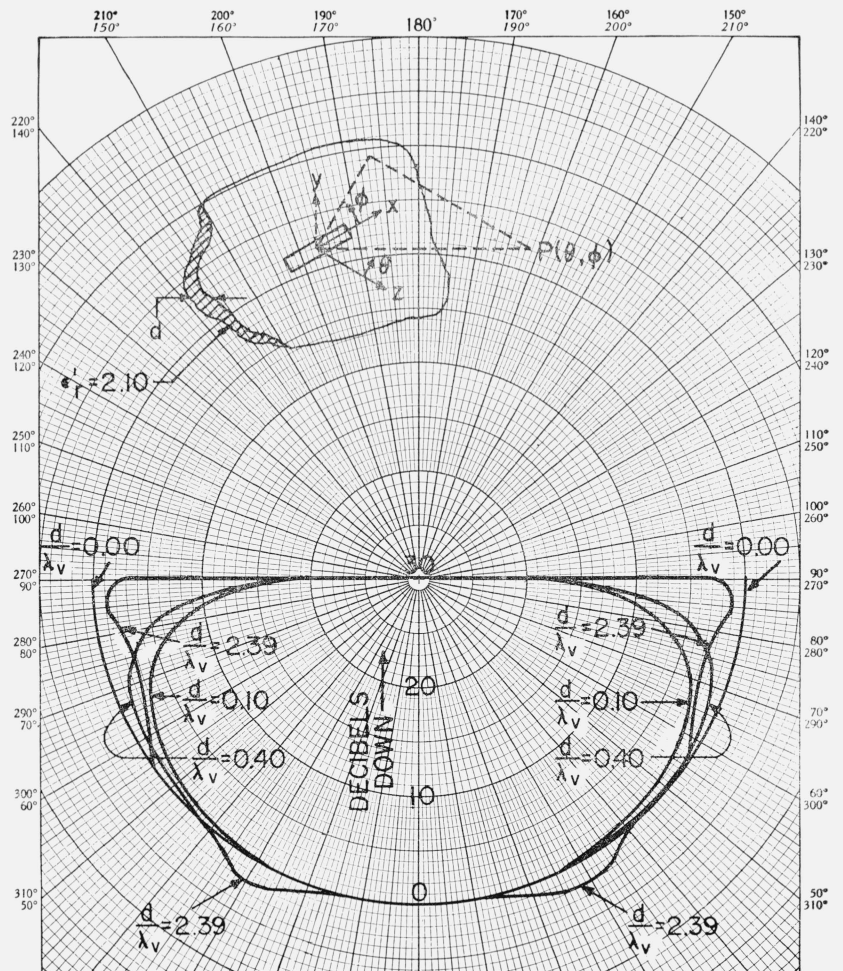
# 4. Numerical Computations—Plasma Coating

Next, consider the case of a neutral, homogeneous, isotropic, linear, lossless plasma coating characterized by a relative dielectric constant of $\epsilon_r' = 1 - 1/p^2$ with $p \equiv f/f_p$, where $f$ is the frequency of the applied electromagnetic field and $f_p$ is the plasma frequency. For this case the $\theta$ polarization pattern relationships become for the exciting frequency greater than or equal to the plasma frequency ($p \geq 1$)

$$\left| \frac{E_{\phi \ \text{no plasma}}}{E_{\phi \ \text{plasma}}} \right|^2 = |g|^{-2} = \begin{cases} \dfrac{p^2 c^2\theta - c^2(\Delta\sqrt{p^2 c^2\theta - 1})}{p^2 c^2\theta - 1}, & 0 \leq \theta \leq \theta_0, p \geq 1 \\[4mm] \dfrac{\cosh^2(\Delta\sqrt{1 - p^2 c^2\theta} - p^2 c^2\theta}{1 - p^2 c^2\theta}, & \theta_0 \leq \theta \leq \theta_m, p \geq 1 \end{cases} \tag{22}$$

where $\theta_0 \equiv \text{arc } c\left(\dfrac{1}{p}\right)$, $\Delta \equiv \dfrac{\omega_p d}{C}$, $C$ is the speed of light in vacuum, and $\theta_m = \text{arc } c\left(\dfrac{d}{r}\right) < \pi/2$. (Only the $\phi$ polarization will be considered for reasons which will be made clear in the discussion of experimental results.) When the operating frequency is below or equal to the plasma frequency, $p \leq 1$, then

$$\left| \frac{E_{\phi \ \text{no plasma}}}{E_{\phi \ \text{plasma}}} \right|^2 = |g|^{-2} = \frac{\cosh^2(\Delta\sqrt{1 - p^2 c^2\theta} - p^2 c^2\theta}{1 - p^2 c^2\theta} \qquad 0 \leq \theta \leq \theta_m, p \leq 1. \tag{23}$$

The effect of the plasma coating on the on axis ($\theta = 0$) field strength is obtained from these equations, and is as shown in figure 3a. The attenuation shown is for a constant level of aperture excitation, i.e., it does not include the attenuation due to the impedance mismatch caused by the sheath. It is seen that for $\Delta \gtrsim 1$ corresponding to a high $\omega_p$ for a fixed $d$ or a
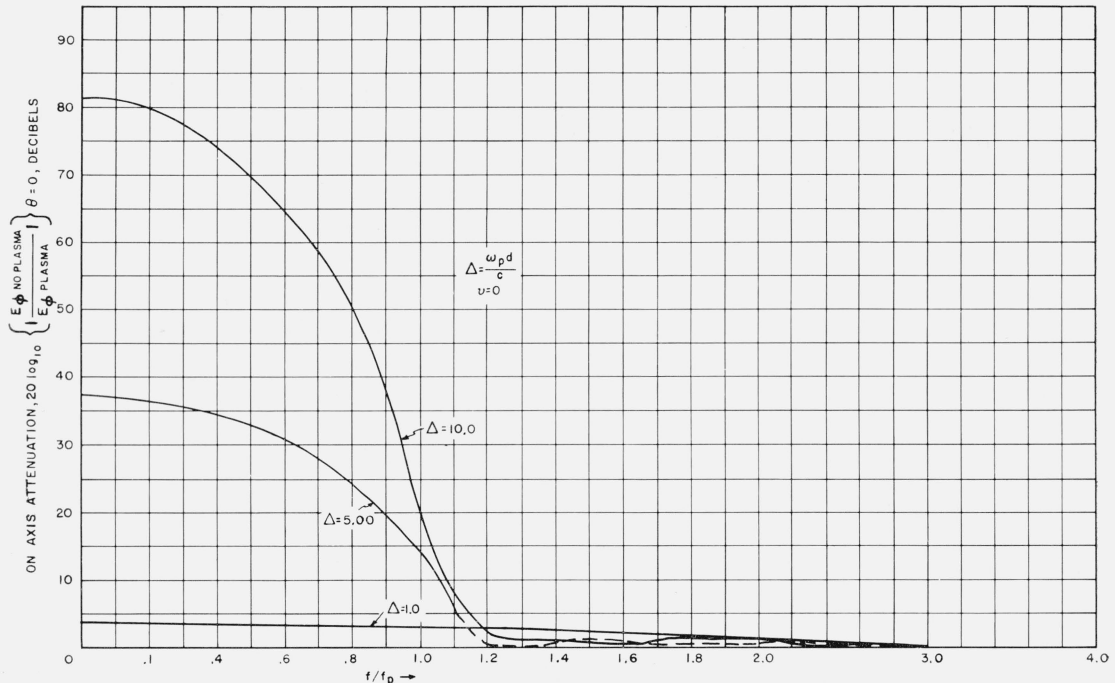


FIGURE 3a.  *On axis attenuation of radiation field due to plasma sheath of constant excitation.*
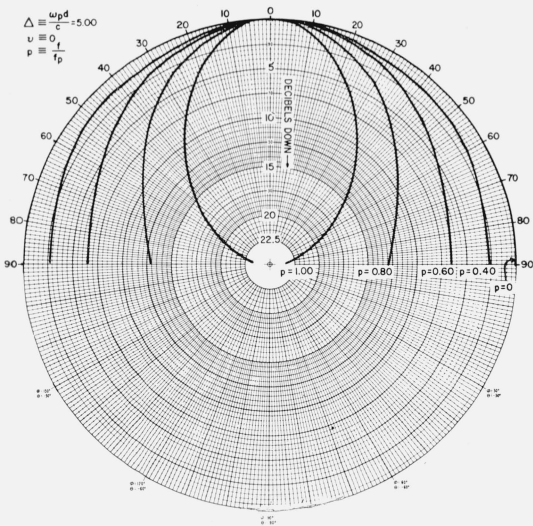
FIGURE 3b. *Plasma sheath effect on φ polarization radiation power pattern, f ≤ f_p.*
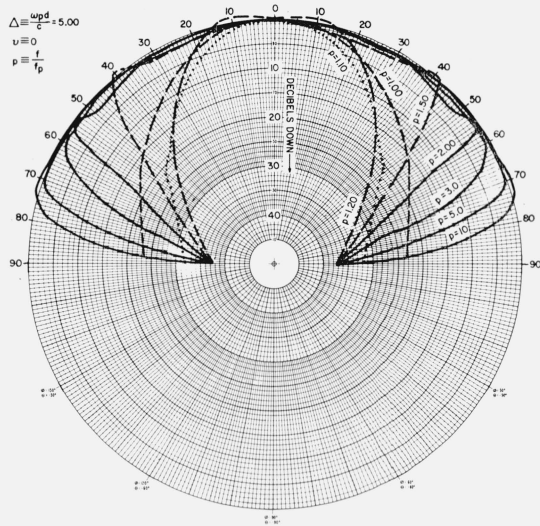
FIGURE 3c. *Plasma sheath effect on φ polarization radiation power pattern, f ≥ f_p.*

large $d$ for a fixed $\omega_p$, that the attenuation introduced can be quite severe for $f \leq f_p$. For a $\Delta$ of 10 the attenuation is much too large to be tolerable in a practical radiating system, whereas for $\Delta = 1$, very little effect occurs. As a compromise, a plasma parameter value of $\Delta = 5.00$ was chosen to determine the effect of the plasma on pattern shape. Using (22) and (23) the change in the shape of the $E_\phi$ polarization power pattern due to the presence of a plasma of $\Delta = 5$ was determined, and is shown in figures 3b and 3c, which are plots of $20 \log_{10} \left| \dfrac{g(0)}{g(\theta)} \right|$. These patterns give the relative change in the power radiation patterns of the uncoated antenna due to the presence of the plasma.

From the patterns, it is seen that for $f$ approaching $f_p$ the presence of the plasma tends to appreciably sharpen the radiation pattern and as $f$ deviates far from $f_p$ either far above it ($p \gg 1$) or far below it ($p \approx 0$) the pattern is affected very slightly except for $p \gg 1$ and $\theta$ approaching the ground plane.

## 5. Experimental Results

To see how well the above theoretical solution for an infinite ground plane can be used to predict the radiation fields from a slot on a finite ground plane, the radiation patterns for the cases of the thin $\left( \dfrac{d}{\lambda_v} = 0.10 \right)$ and medium $\left( \dfrac{d}{\lambda_v} = 0.40 \right)$ Teflon coatings were experimentally measured. The ground plane chosen was a circular disk 18 in. in diameter (approximately 15 free-space wavelengths at the frequency used). Three such disks were made, one noncoated, one with ⅛ in. Teflon coating, and one with ½ in. Teflon coating, corresponding to $\dfrac{d}{\lambda_v} = 0.00$, 0.10, and 0.40, respectively, at a frequency of 9.43 Gc/s. Each disk was excited by a half wavelength resonant slot at this frequency $\left( x_0 = \dfrac{\lambda_v}{2} = 0.625 \text{ in.} \right)$. The slot width was chosen to be a tenth of a free-space wavelength ($y_0 = 0.125$ in.). A photograph of one of the disks and the exciting waveguide is shown in figure 4a. The antennas were used in a receiving position and were tuned for maximum response with a slide screw tuner, which excited a crystal which in turn fed an Ant-Lab polar recorder. A 6 in. pyramidal horn was used as the transmitting source in conjunction with a Hewlett Packard-620A Signal Generator. The distance between receiving and transmitting antennas was approximately 20 ft. The pertinent patterns taken in the horizontal ($xz$) plane for all the cases are shown in figure 4b,

371
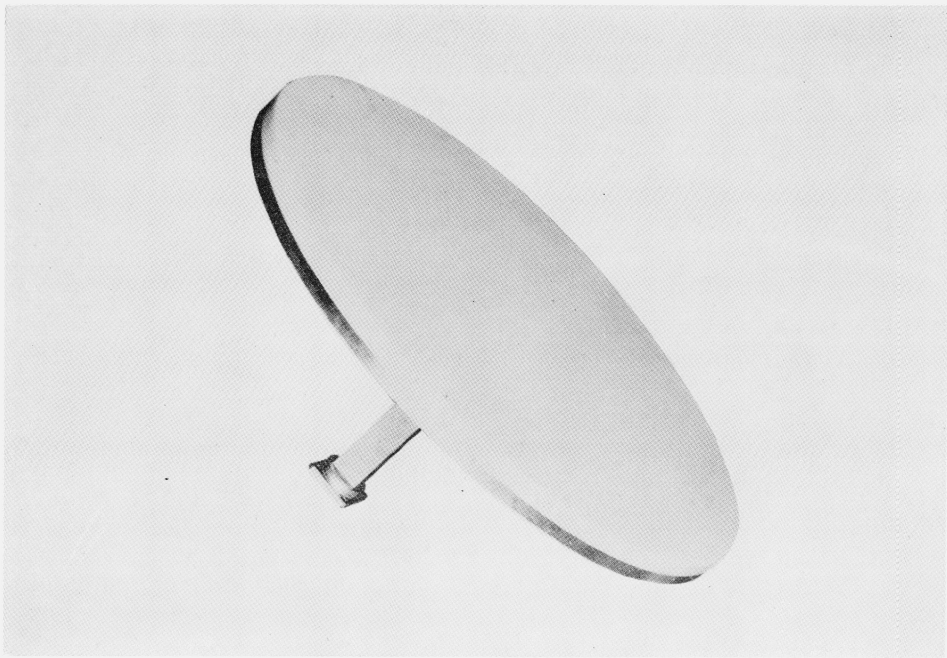
FIGURE 4a.   *Dielectric coated antenna.*
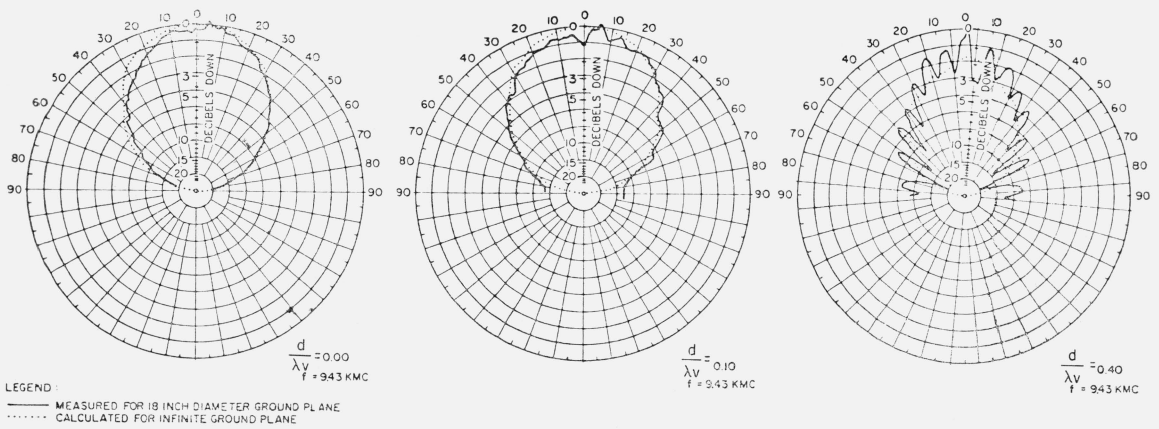
FIGURE 4b.   *Power radiation patterns in horizontal plane.*
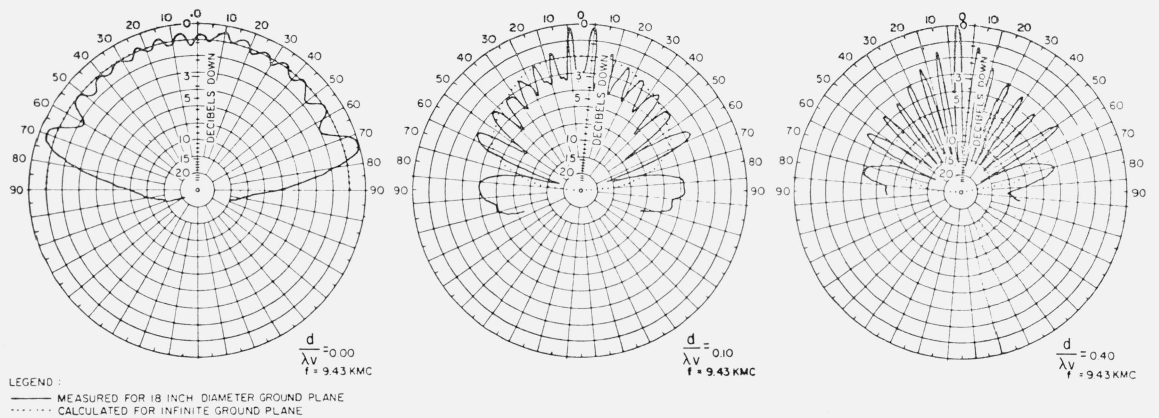
FIGURE 4c.   *Power radiation patterns in vertical plane.*

and those in the vertical $(yz)$ plane in figure 4c. The calculated patterns for the infinite ground plane are also shown on these figures for ease of comparison.

To obtain a realistic comparison between the calculated infinite ground plane patterns and the measured patterns, the calculated patterns were drawn in the following way. First it is known that the calculated fields from the noncoated infinite plane are correct, and yet figure 4c for the case $d=0$ reveals that the vertical pattern is not a semicircle, but tends to oscillate about a mean value, then approaches zero at $\theta = \pm 90°$. This effect for this noncoated case can be attributed to one or both of two reasons: (1) a finite slot height causes a slot field distribution different from that assumed, and (2) the finite diameter ground plane.

The horizontal plane pattern measured agrees well with the calculated pattern, hence the former reason is probably not predominant. The mean value of the vertical plane pattern at $\theta = 0$ was obtained and used as the reference point through which the calculated pattern was drawn. The same procedure to locate the reference point at $\theta = 0$ was used for all the other patterns.

Figure 4b depicts the very good agreement in the horizontal planes for the cases $\frac{d}{\lambda_v} = 0.00$ and 0.10 obtained. The measured pattern in this plane for the case of $\frac{d}{\lambda_v} = 0.40$ oscillates somewhat about the calculated values. These oscillations are observed to be more severe than for the uncoated case in the horizontal plane. Figure 4c, which depicts patterns in the vertical plane, reveals that the calculated values for the infinite ground plane serve as a mean value of the measured patterns for the finite ground plane. It is seen that as the coating thickness is increased, the oscillations about the calculated values become much more severe. In particular, for the case $\frac{d}{\lambda_v} = 0.40$, extremely severe oscillations were measured; enough to make the patterns predicted by the theoretical infinite plane model unusable. This is attributed to the edge effects and the finite size of the ground plane. From this observation it is seen that the interference effects are definitely a function of the dielectric thickness indicating, apparently, that the energy is stored within the dielectric and also radiated from the edge. The deviation of the observed patterns from those predicted by the uncoated infinite ground plane solution is attributed in part to the finiteness of the ground plane and in part to the presence of the coating, especially since the deviation is not so noticeable in the absence of the coating. It is noticed that the same number of lobes (15) appears for each case, except for the $\frac{d}{\lambda_v} = 0.10$ case where the center lobe splits. It is to be noted that this number of lobes is about the same as the diameter of the ground plane expressed in terms of free-space wavelengths.

Thus, whereas the horizontal plane patterns of the finite coated ground plane can be predicted fairly well using the solution for the infinite coated plane model, the same is not true for the vertical plane patterns.

## 6. Effect of Finite Ground Plane on Radiation Patterns

To account for the preceding deviation between the observed vertical plane patterns of the finite ground plane and those predicted for the infinite plane model, the following methods can be used.

### 6.1. Uncoated Ground Plane

The finite size of the ground plane along the $y$ axis causes an abrupt discontinuity in the electric field at the edges of this plane which are parallel to the long dimension of the slot, since the normal component of this field will be discontinuous at its surface but continuous in the space immediately exterior to it. Because of this discontinuity, there will be diffracted or scattered waves produced at these edges. This discontinuity does not exist along the $x$ axis and hence no scattering will occur at the edges of the ground plane perpendicular to the long dimension of the slot.

The effect of these scattered waves has been treated by placing equivalent image radiators at the edges, which are parallel to the long dimension of the slot, and superimposing their radiation with that produced by the slot to obtain the total radiated field [Dorne and Lazarus, 1947]. However, this method requires a knowledge of the strength of these image fields which can, however, only be determined after the pattern is measured. Hence, this method can only describe, not predict, the patterns.

A more satisfactory treatment considers the slot as a receiving element, and in conjunction with the known Sommerfeld diffraction effects produced about the edges by an incident plane wave, computes the voltage induced across the slot by this wave and then uses reciprocity. This has been done with success to predict the vertical plane patterns produced by slots in uncoated rectangular metal plates [Frood and Wait, 1956].

However, the most rigorous treatment to date to predict the patterns produced by a slot in a finite rectangular metal plane is that which represents the plate as the limiting case of an infinitesimally thin elliptic metal cylinder [Wait, 1955; Wait and Walpole, 1955; Wait and Mientka, 1958; and Wait, 1959]. Related work [Wait and Conda, 1957a] for the half plane has also been reported.

Now, although the experiments in this paper were performed for a circular, not rectangular, ground plane it can be argued that the effect of the finite size of the ground plane on the pattern in the vertical plane should still be primarily determined by the length of the ground plane (as measured between the edges parallel to the long dimension of the slot), especially if the ground plane is much larger than the slot, as is the case. As such, Wait's thin ellipse method is adopted.

Thus, using Wait's result, eq (322) of Wait (1959) it is seen that the $E_\theta$ field produced by the slot in the uncoated finite ground plane is related to that produced by the same slot, but in an infinite uncoated metal plane by

$$\frac{E_\theta(r, \theta, \pi/2)}{E_\theta(r, \theta, \pi/2)|_{D=\infty}} = T(g, \theta), \qquad -\pi/2 \leq \theta \leq \pi/2 \tag{24}$$

where

$$T(g, \theta) \approx \{ F[\sqrt{2g}s(\theta'/2)] + F[\sqrt{2g}c(\theta'/2)] - 1 \} \tag{25}$$

where $\theta' = \pi/2 - \theta$, and $g = \beta_v D/2$, where $D$ is the diameter of the ground plane, and with the function $F$ defined by

$$F[W] = \sqrt{j/\pi} \int_{-\infty}^{W} e^{-ju^2} du. \tag{26}$$

It is noted that if $D \rightarrow \infty$, i.e., if the ground plane is allowed to become infinite, then $T$ becomes unity.

The factor $T(g, \theta)$ can be simplified to

$$|T|^2 = (X^2 + Y^2)/2 \tag{27}$$

where $X = C(x_1) + C(x_2)$ and $Y = S(x_1) + S(x_2)$ with $C(x) = $ cosine Fresnel integral $= \int_0^x c[(\pi/2)$ $u^2]du$, and $S(x) = $ sine Fresnel integral $= \int_0^x s[(\pi/2)u^2]du$, where $x_1 = 2\sqrt{D/\lambda_v}s(\theta'/2)$ and $x_2 = 2\sqrt{D/\lambda_v}$ $c(\theta'/2)$. For the antennas used $D/\lambda_v = 14.37$. A plot of $10 \log_{10} \left[ \frac{|T|^2_{\theta=0}}{|T|^2} \right]$ is shown in figure 5a, which also shows the experimentally measured vertical plane pattern for the uncoated ground plane (i.e., figure 4c, $d=0$ is redrawn). The agreement with the observed pattern and that predicted using Wait's result (24) is seen to be very good.

## 6.2. Coated Ground Plane

It would now be desirable to extend Wait's method of the limiting case of the thin ellipse to the coated case. This requires a solution to the fields produced by a slot on a coated elliptic cylinder which is, however, not currently available.
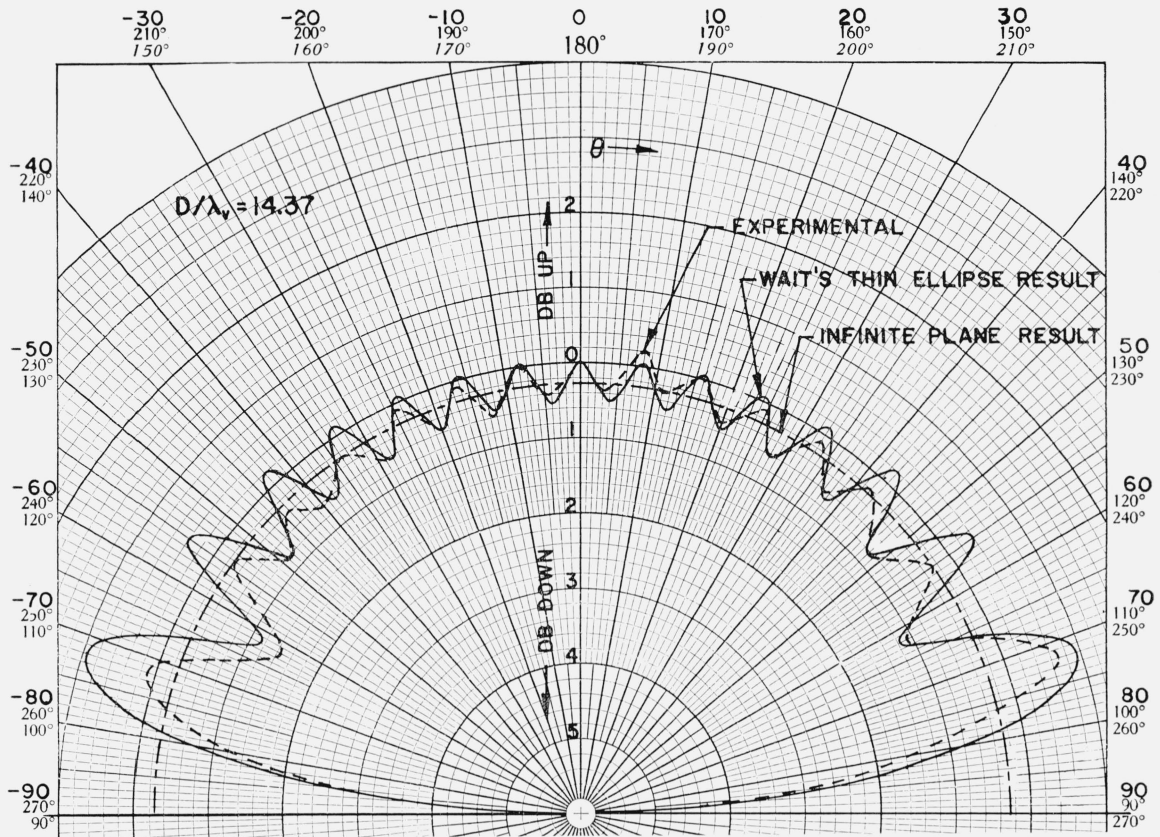
FIGURE 5a. *Experimental and calculated vertical plane power radiation patterns.*

For this reason, either the aforementioned image theory of Dorne and Lazarus or an extension of the work of Sommerfeld to diffraction around a coated edge must be used. The latter method is perhaps more difficult to obtain than the fields from a coated ellipse. Hence, if any effort is to be expended on determining the effect of a finite, coated, ground plane, it is probably preferable to obtain the fields from a coated ellipse and use Wait's more rigorous method. However, to obtain a qualitative idea of the effect of a coated ground plane, the method of Dorne and Lazarus is adopted, despite its limited ability to describe, not predict. Thus, image sources of strength $k$ are placed at the edges of the ground plane, and referring to figure 5b, the field is to be computed at a point $P$ far removed from the slot at an angle $\theta$ from the $z$ axis which is perpendicular to the ground plane. The existence of a field $k\mathbf{E}_0 e^{j\omega t}$ is postulated at the edges where $k$ is a number, in general complex, and less than unity, and $\mathbf{E}_0$ is the source field at the slot. For the case of no coating, $|k| \ll 1$, but with a coating the magnitude of $k$ can increase, since the coating tends to trap or store energy, and less will be radiated outward from the coating as the wave traverses the distance from the slot to the edges of the ground plane. From figure 5, the field at $P$ is $\mathbf{E} = \mathbf{E}_0 e^{j\omega t}(e^{-j\beta_v r} + k e^{-j\beta_v r_1} + k e^{-j\beta_v r_2})$, where $r_1 = r + (L/2)s\theta$, and $r_2 = r - (L/2)s\theta$. Therefore, $\mathbf{E} = \mathbf{E}_0 e^{j(\omega t - \beta_v r)}[1 + 2kc(\beta_v s\theta L/2)]$.

Now, it can be conjectured that $k = |k| e^{-j\beta_v (L/2)\sqrt{\overset{v}{\epsilon_r}}}$ where $\overset{v}{\epsilon_r}$ is the relative dielectric constant of the coating. This conjecture is arrived at by considering the wave to travel from the slot to the image-source location with the propagation constant of the coating material. Hence, in general, $k$ will be complex. For the experiments conducted ($\overset{v}{\epsilon_r} = 2.10$, $f = 9.30$ Gc/s, $L = 18$ in.), hence $\beta_v (L/2)\sqrt{\overset{v}{\epsilon_r}} \approx 20\pi$ and, therefore, $k$ is approximately pure real and positive. For this
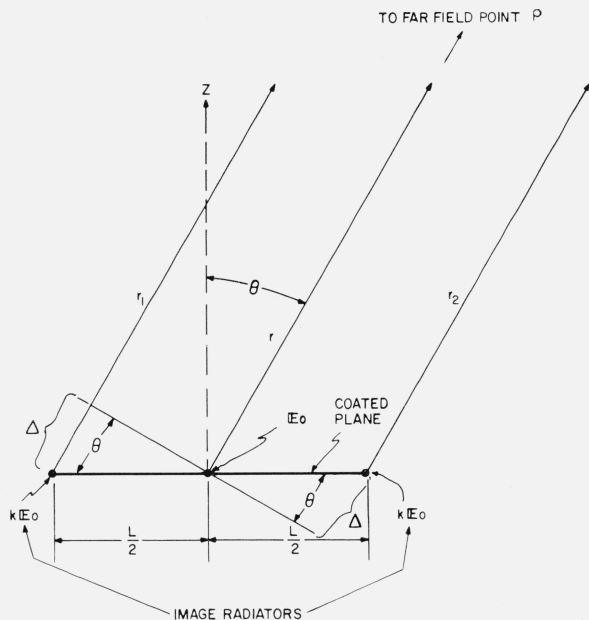
375

case, inspection reveals that the maximum and minimum values of $|\mathbf{E}|$ are $|\mathbf{E}_{\max}|=|\mathbf{E}_0|$ $(1+2k)$ and $|\mathbf{E}_{\min}|=|\mathbf{E}_0|(1-2k)$ where the maximum points, lobes, occur at the angles $\theta_n$ given by

$$s\theta_n = \frac{2(n-1)}{\left(\dfrac{L}{\lambda_v}\right)}, \qquad n=1,2,3,\ldots. \tag{28}$$

The ratio of powers at the maximum and minimum points is then

$$\frac{|\mathbf{E}_{\max}|^2}{|\mathbf{E}_{\min}|^2} = \left(\frac{1+2k}{1-2k}\right)^2. \tag{29}$$

From figure 4c of the text for the thick coating case $(d/\lambda_v=0.40)$ it is seen that this ratio was measured to be about 15 db, corresponding to (from (29)) $k\approx0.35$. Using (28), the calculated locations of the lobes for this case are as tabulated in table 1. It is seen that these locations correspond quite well to those measured, and that in the region $0° \leq |\theta| < 90°$, 15 lobes are predicted by the image theory, as also was measured.

For the cases of a thin coating or no coating, there is very little energy trapping and $k$ will then be very small, $k \ll 1$. However, the lobe location and therefore number, will still be governed by (28) which also agree very well with the more exact approach of Wait, using the limiting case of an elliptic cylinder. Hence, it is seen that the image theory of Dorne and Lazarus can be extended to apply to the case of the coated ground plane by merely increasing the value of $k$ to take into account the increased trapping of energy effect due to the coating. For any particular case, one should be able to determine a value of $k$, in general complex, so as to describe the observed pattern. Unfortunately, this method cannot predict $k$ before the pattern is observed.

## 7. Conclusions

The radiation fields produced by a specified, tangential, electric field distribution in an arbitrarily shaped aperture cut in an infinite coated metal plane have been found by the Fourier transform method of J. R. Wait, and are given by (14) and (15). Experimental results for the case of a slot in a Teflon coated finite metal plane indicate that the infinite plane model can be used to predict the radiation patterns quite well in the plane of the slot (horizontal

TABLE 1. *Lobe locations*

| n | $\theta_n{}^\circ$ |
|---|---|
| 1 | 0. |
| 2 | 7.96 |
| 3 | 17.20 |
| 4 | 24.5 |
| 5 | 33.7 |
| 6 | 43.8 |
| 7 | 56.2 |
| 8 | 75.5 |

plane) but not in the plane perpendicular to the slot (vertical plane). The patterns in the vertical plane (for the noncoated case) can, however, be predicted quite well by the method of Wait which treats the finite plane as a limiting case of a thin ellipse. Presumably, this method could also be used to predict the vertical plane patterns for the coated case. However, since the solution for the radiation fields from a coated ellipse are as yet unavailable, this must be left for future work.

As such, an empirical image theory which is less rigorous than Wait's ellipse method is used to describe the vertical pattern, for the coated case, and shows that severe oscillations occur due to reflection at the edges of the ground plane and apparent trapping of energy by the coating (since the severity of oscillations increases with the coating thickness).

Calculations of the horizontal plane radiation pattern for the case of a lossless plasma coating indicate that the pattern shape can be considerably sharpened, at the expense of some attenuation, when the plasma frequency is near or equal to the operating frequency.

The near field and input admittance of an aperture in an infinite coated metal plane can be found by evaluating the Fourier transform coefficients in the near field and taking their appropriate inverse transforms. This is planned for a future companion paper.

————

## 8. References

Cohn, G. I., and G. T. Flesher (1958), Theoretical radiation pattern and impedance of flush-mounted coaxial aperture, Proc. Nat. Electron. Conf. **14**, 150–168 (Chicago, Ill.).

DiFrancia, G. Toraldo (1955), Electromagnetic waves, pp. 36–38 (Interscience Publishers, Inc., New York, N.Y.).

Dorne, A., and D. Lazarus (1947), Very high frequency techniques, ch. 7, 174–177, Slot Antennas (McGraw Hill Book Co., Inc., New York, N.Y.).

Frood, D. G., and J. R. Wait (Jan. 1956), An investigation of slot radiators in metal plates, Proc. Inst. Elec. Engrs. **103**, pt. B, No. 1, 103–110.

Knop, C. M. (Nov. 1961), The radiation fields from a circumferential slot on a metal cylinder coated with a lossy dielectric, IRE Trans. Ant. Prop. **AP–9**, No. 6, 535–545.

Wait, J. R. (Apr. 1955), Field produced by an arbitrary slot on an elliptic cylinder, J. Appl. Phys. **26**, No. 4, 458–463.

Wait, J. R. (1959), Electromagnetic radiation from cylindrical structures (Pergamon Press, New York, N.Y.).

Wait, J. R., and A. M. Conda (Oct. 1957a), The pattern of a slot-array antenna on a finite and imperfect ground plane, Proceedings of Congres International Circuits et Antennas Hyperfrequencies, Paris, France, **1,** 21–29 (Supplement special a' l'onde Electrique, Août 1958, No. 376 bis).

Wait, J. R., and A. M. Conda (Nov. 1957b), Radiation from dielectric clad and corrugated cylinders, J. Res. NBS **59,** No. **6,** 307–316.

Wait, J. R., and W. E. Mientka (June 1957), Slotted cylinder antennas with a dielectric coating, J. Res. NBS **58,** No. **6,** 287–296.

Wait, J. R., and W. E. Mientka (1958), Calculated patterns of slotted elliptic-cylinder antennas, Appl. Sci. Res. (The Hague), Sec. B, **7,** 449–462.

Wait, J. R., and R. E. Walpole (May 1955), Calculated radiation characteristics of slots in metal sheets, Can. J. Technol. **33,** No. 3, 211–227.

## 9. Additional References

Hodara, H. (Jan. 1963), Radiation from a gyro-plasma sheathed aperture, IEEE Trans. Ant. Prop., **AP-11,** No. 1, 2–12.

Hodara, H. and G. I. Cohn (Sept. 1962), Radiation from a gyro-plasma coated magnetic line source, IRE Trans. Ant. Prop., **AP-10,** No. 5, 581–593.

Yeh, C. (Sept. 1962), The external field produced by an arbitrary slot on a dielectric coated elliptic cylinder, University of Southern California, USCEC Report 82–206, EE–16, AFCRL 62–781.

(Paper 68D4–354)